ELSEVIER

Journal of Wind Engineering
and Industrial Aerodynamics 94 (2006) 659–673

JOURNAL OF wind engineering AND industrial aerodynamics

www.elsevier.com/locate/jweia

A wind-tunnel study on exhaust-gas dispersion from road vehicles—Part II: Effect of vehicle queues

Isao Kanda[a,*], Kiyoshi Uehara[a], Yukio Yamao[a], Yasuo Yoshikawa[b,1], Tazuko Morikawa[b]

[a]*National Institute for Environmental Studies, 16-2 Onogawa, Tsukuba 305-8506, Japan*
[b]*Petroleum Energy Center, 4-3-9 Toranomon, Minato-ku, Tokyo 105-0001, Japan*

Received 1 December 2004; received in revised form 6 September 2005; accepted 20 June 2006
Available online 2 August 2006

Abstract

By a reduced-scale wind-tunnel experiment, we investigate the dispersion behavior of exhaust gas from automobiles. Based on the results of single-vehicle cases in Part I of our work, we consider vehicle queues consisting of passenger cars (P) and small-size trucks (T). The roles of the vehicles before and after the gas-emitting vehicle are as follows. By their turbulent wake, the preceding vehicles make the concentration field approximately symmetric in the spanwise direction despite the significant lateral offset of the exhaust pipe. The vehicles behind the gas-emitter expand the exhaust plume considerably in the spanwise direction; T expands the plume also in the vertical direction in its roll-up wake, while P scoops up the oncoming plume only around the centerline. For vehicle queues of mixing ratio $P : T = 2 : 1$, the concentration fields when one of the component vehicles emit the gas are measured. It turns out that the plume shape is determined mostly by the type of the gas-emitting vehicle whereas the type of the following vehicles has minor effect. We also present an analytical procedure to approximate the overall contribution from all the queue-forming vehicles by a Gaussian line-source plume formula.
© 2006 Elsevier Ltd. All rights reserved.

Keywords: Air pollution; Traffic emissions; Wind tunnel; Gaussian plume; Eddy viscosity

*Corresponding author. Tel.: +81 29 850 2765; fax: +81 29 850 2580.
E-mail address: kanda.isao@nies.go.jp (I. Kanda).
[1]Nissan Research Center, 1 Natsushima-cho, Yokosuka 237-8523, Japan.

0167-6105/$ - see front matter © 2006 Elsevier Ltd. All rights reserved.
doi:10.1016/j.jweia.2006.06.002

1. Introduction

Traffic-produced turbulence plays an important role in the dispersion of automobile exhaust gas. It is especially the case in the congested traffic in urban areas. However, the nature of traffic-produced turbulence is poorly understood, and the existing air pollution models adopt various empirical schemes that are difficult to verify.

In order to clarify the role of moving vehicles, our previous paper ([1], K1 hereinafter) investigated the relationship between the velocity field and the dispersion behavior for single-vehicle configurations by a reduced-scale wind-tunnel experiment. For simplicity, we assumed no ambient wind and no heat flux from the vehicle engines. Unlike other experimental works, the buoyancy of the exhaust gas was simulated. We found that the exhaust-gas concentration field conforms to the wake velocity field behind the vehicles and that the buoyancy has relatively small effect.

In urban areas, vehicles usually form queues, and the effect of other vehicles needs to be incorporated. The preceding vehicles induce turbulence in the ambient, which otherwise is stationary under our assumption of no ambient wind; the following vehicles expand and/or deflect the exhaust plume in both the horizontal and the vertical directions. We note that such complications are absent when the vehicle interval is sufficiently large as on highways in USA ([2]).

In this paper, we extend our previous work to multiple-vehicle configurations. The effects of preceding and following vehicles are examined in Sections 3 and 4, respectively, for passenger cars. A particular case of a mixed composition queue is investigated systematically in Section 5. We also present an analytical procedure to evaluate the overall effect of the mixed queue in Section 5.2.

2. Experimental method

The experimental method is briefly described here. The details are given in K1.

We model a traffic condition representative of the Tokyo metropolitan area. A 12-hour traffic survey was conducted on a weekday around Kamiuma intersection (Setagaya, Tokyo) where the national highway 246 and the ring road No. 7 crosses. We found that the traffic consists mostly of passenger cars (P) and small-size trucks (T). Hence, vehicle queues formed by these two types are tested. The observed mixing ratio was $T/(T+P) = 0.3\sim0.4$. Hence, the mixing ratio is set as $P:T=2:1$. In the survey, various driving parameters were monitored for five drivers on a sedan-type passenger car. The vehicle speed varied widely and there was no particular speed with outstanding frequency (cf. Fig. 1 in K1). For experimental convenience, we select $20\,\mathrm{km\,h^{-1}}$ ($5.56\,\mathrm{m\,s^{-1}}$). Fig. 1 shows the dependence of the tail-to-head interval on the vehicle speed. On average, the interval can be expressed as

$$\text{Interval (m)} = 0.47 \times (\text{Vehicle speed } (\mathrm{km\,h^{-1}})) + 3.2.$$

At $20\,\mathrm{km\,h^{-1}}$, this formula leads to 12.6 m. This interval, however, is the average for all the preceding vehicles, and vehicle-type specific values could not be obtained. Expecting that a passenger car following a truck would keep a longer interval for better front view, we set the interval behind P and T as 10 and 20 m, respectively. As in K1, we assume no ambient wind and no heat flux from engines.

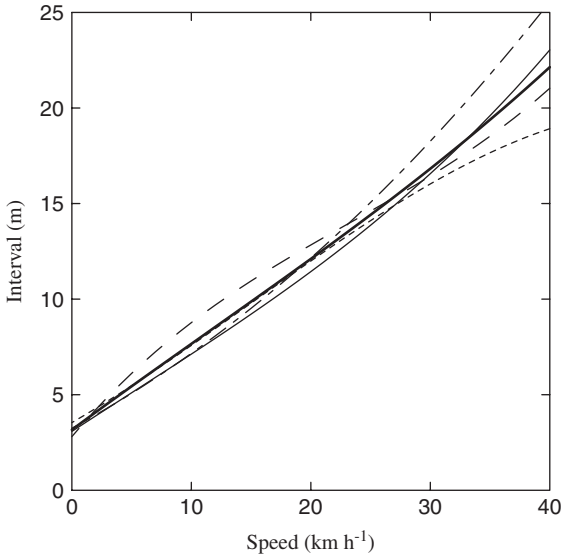

Fig. 1. Dependence of the tail-to-head interval on the vehicle speed. The thin lines represent the data along the four routes branching from Kamiuma intersection, and the thick line is the average. All the data are averages for five different drivers.

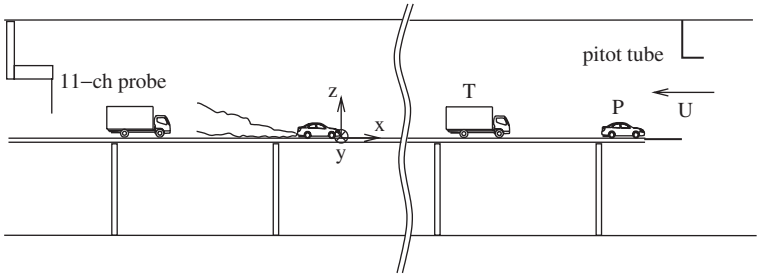

Fig. 2. A schematic view of an experimental configuration (not to scale). P stands for passenger car and T for small-size truck.

Instead of vehicles moving into a still ambient, we study an approximately equivalent configuration of a low-turbulence wind blowing against stationary vehicles. The model size is $\frac{1}{20}$ of the real scale. The lengths of the model P and T are 225 and 304 mm, respectively.

The wind speed is $U = 1.5\,\mathrm{m\,s^{-1}}$ beyond and including which the mean-flow pattern around the vehicles is independent of the Reynolds number. For this wind speed, the buoyancy of the exhaust gas is determined by matching the Froude number based on either the wind speed or the exhaust emission speed. The buoyancy is controlled by the ratio of helium in the tracer gas. The emission speed V is determined by matching the ratio of the inertia of the ambient wind to that of the exhaust gas.

Fig. 2 shows an experimental configuration. The model vehicles are placed on a table with a 1 mm-thick plate at the upwind edge in order to minimize the effect of the boundary

layer on the ground (table top). The Cartesian coordinate system is defined with the origin at the head of the gas-emitting vehicle ($x = 0$), at the centerline ($y = 0$), and on the table top ($z = 0$). The vehicle queue is denoted by the order from the upwind vehicle, with the gas-emitting vehicle marked by an asterisk. The queue in Fig. 2, for example, is denoted as $P_1 T_2 \ldots P_n^* T_{n+1}$.

The tracer gas is a mixture of ethane, helium and nitrogen, and is emitted from one of the vehicles. The concentration of ethane is measured by a 12-channel flame ionization detector (Kimoto Electric Co., Ltd.). The data are presented by the measured raw values in ppm.

3. Effect of preceding vehicles

We examine the concentration field when there are m vehicles in front of the gas-emitting vehicle and no vehicles behind, and determine the critical number M at which further addition of vehicles does not alter the concentration field. The vehicle type tested is P. The critical number M thus determined can represent the effect of infinitely long preceding queue.

Fig. 3 shows the yz section of the concentration field at 300 mm behind the rear bumper of the gas-emitting vehicle with $m = 0, 1, 2, 3$ preceding vehicles. The contours are biased to negative y because the exhaust pipe is at $y = -25$ mm.

At low z, the bias magnitude changes considerably from $m = 0$ (Fig. 3(a); about -40 mm) to $m = 1$ (Fig. 3(b); about -25 mm). Similar reduction of lateral bias at low z is observed for T (cf. Section 5.1). A possible cause is the slightly more raised wake streamlines when there are preceding vehicles than when there are none (cf. Sections 3.1, 3.2 of K1): larger portion of the exhaust plume is carried to the region of large velocity fluctuation. However, since a significant bias also exists behind a single T without preceding vehicles even though a T has a conspicuous roll-up wake, the raised streamlines are unlikely to be the major cause. Instead, we suppose that the relatively large eddies generated by the preceding vehicles enhance mixing at low z and reduce the lateral bias.

For $m = 2$ (Fig. 3(c)), the concentration field changes slightly from $m = 1$, and the results of $m = 2$ and 3 (Fig. 3(d)) are almost identical. Hence, the critical number M is 2.

We note that the vertical spread of the exhaust plume is slightly increased by the preceding vehicles, in agreement with the numerical simulation of [3].

4. Effect of following vehicles

We consider a queue of five P's: two P's before and after the gas-emitting $P\ P_1\ P_2\ P_3^*\ P_4\ P_5$. As shown in the previous section, the preceding two P's generate turbulence equivalent to that by an infinitely long queue.

Fig. 4(i) shows the concentration contours in the yz plane at $x = -525$ mm (i-c; 300 mm behind the rear bumper of the gas-emitting P), $x = -1050$ and -1775 mm (i-b, a; 100 mm behind the rear bumper of the first P_4 and the second P_5 following P, respectively). Fig.4(ii) shows the corresponding contours without the following P's. Notable effects of the following vehicles are: (1) the exhaust plume spreads in the y direction, (2) the plume center at low z shifts toward negative y, (3) the concentration at high z is relatively large around $y = 0$.

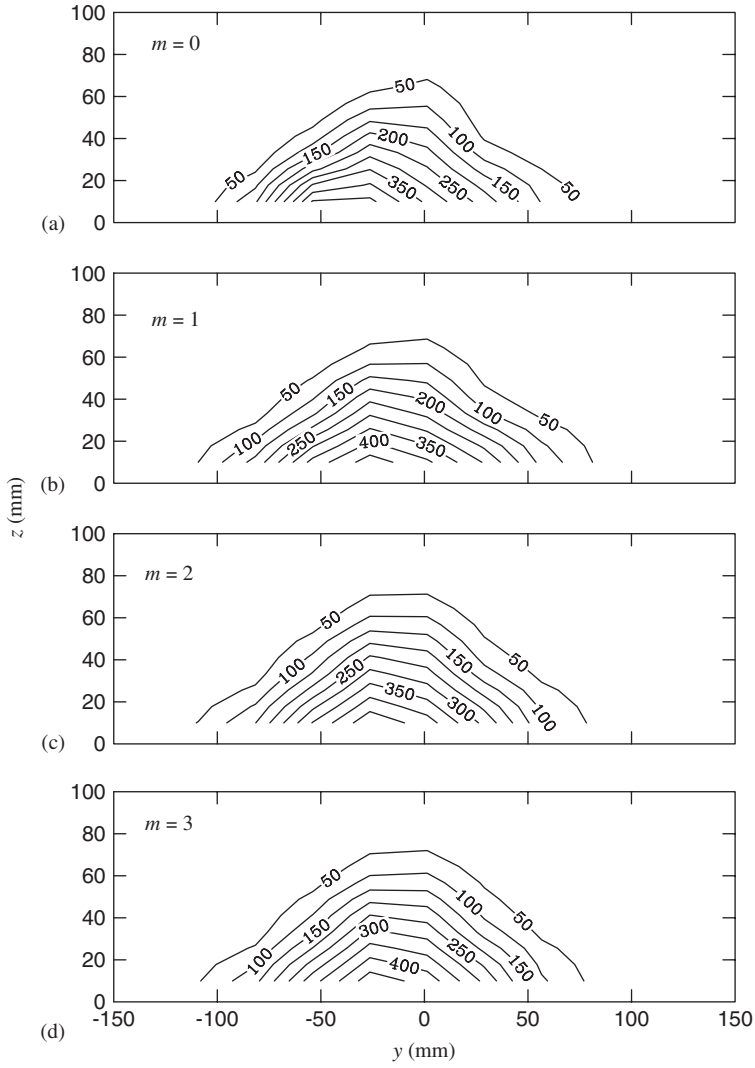

Fig. 3. Concentration contours in the yz plane at $x = -525$ mm (300 mm behind the rear bumper) when there are m P's ahead of the gas-emitting P.

The first feature is due to the relatively flat shape of P and to the relatively low profile of the plume; at the head of a following P, the plume is separated primarily in the horizontal direction, advected alongside the P, and merged in the mixing region of the rear wake. The reason for the second feature is not understood well. It might be a property of a plume impinging asymmetrically on an obstacle, or the flow around the tyres of the following P's could be responsible. The third feature concerns the upper part of the plume that climbs over P. In Fig. 5 showing the streamlines around a P behind nine P's (cf. Section 3.1 of K1), if we follow a streamline from a point ahead of P and a little lower than the top of P, we find that the air is lifted above the top of P and then is brought to the region above the

trunk where both the streamwise and vertical fluctuations are large (cf. Section 3.2 of K1). Hence, the plume lifted due to the streamlined shape of P is mixed at the elevated height and results in the bulge around $y = 0$ in Fig. 4(i-a, i-b).

The climbing behavior of the upper part of the plume can be verified by the concentration field above P. Fig. 6(a), (b) shows the concentration profiles in the y direction at $z = 80$ mm (above the top of P) in the front half (a) and in the rear half (b) of the first following P. The measurement locations are indicated by asterisks in Fig. 5. We observe that the concentration is higher in the rear half than in the front half, contrary to the normal plume behavior that the concentration decays in the downstream direction. However, if we trace back the streamlines from the measurement points, we find that the

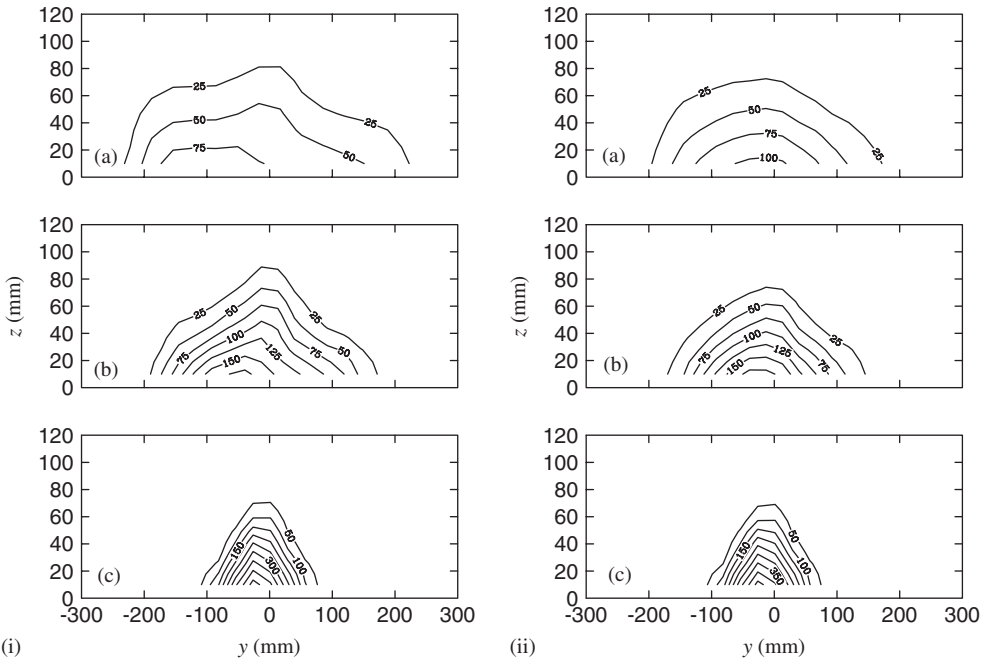

Fig. 4. Concentration contours in the yz plane behind the gas-emitting P preceded by two P's. There are (i) two P's and (ii) no vehicles behind the gas-emitting P. The x (mm) coordinates are (a) −1775, (b) −1050 and (c) −525.

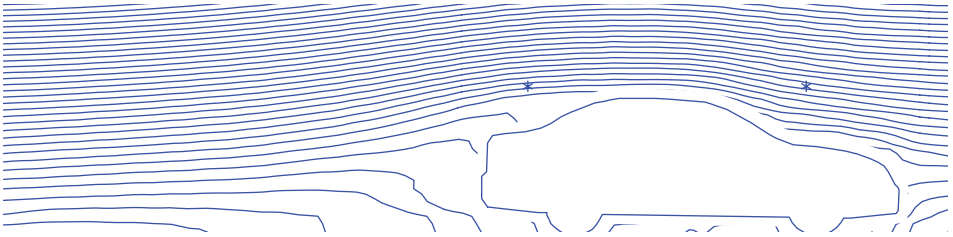

Fig. 5. Streamfunction contours on $y = 0$ around a P behind nine P's, measured by particle image velocimetry (DANTEC Dynamics). The asterisks denote the concentration measurement points in Fig. 6.

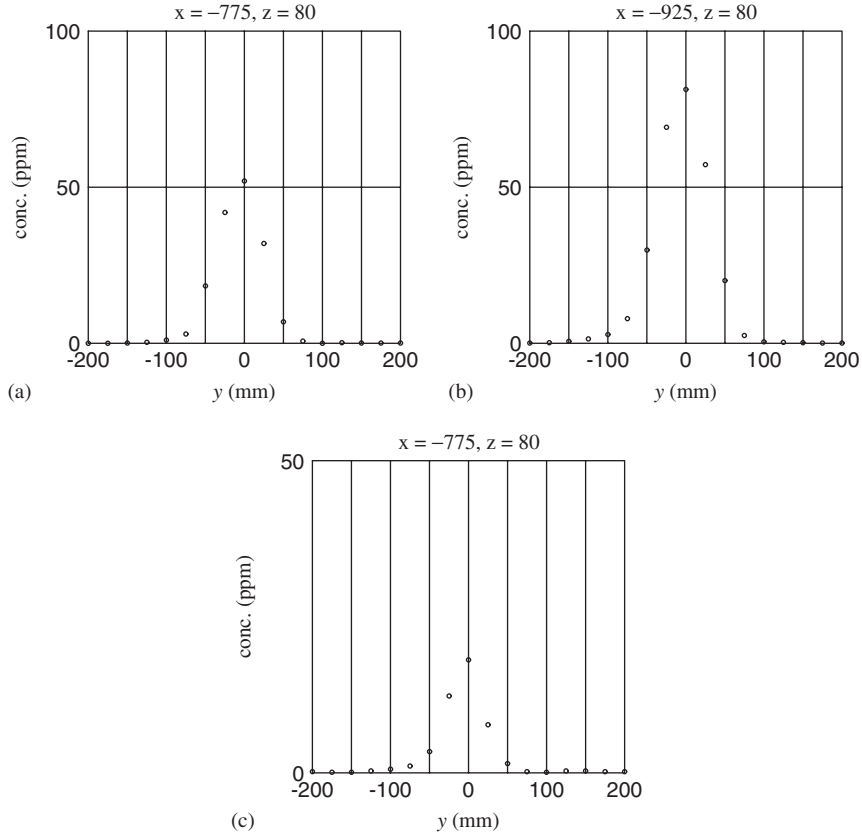

Fig. 6. Concentration profiles along y at points above the first following P (except for (c)) behind the gas-emitting P preceded by two P's. The measurement points are indicated in Fig. 5: (a) in the front half, (b) in the rear half. The sub-figure (c) shows the result at the same point as (a) but without the following P's P_1 P_2 P_3^*.

origin of the streamline through the rear half point is from lower z than that of the streamline through the front half point. Since the concentration in the plume is higher at lower z as shown in Fig. 4, the profiles of Fig. 6(a), (b) are actually consistent with the streamlines. Also, at both the measurement points, the concentration is significantly higher than when there is no following P (P_1 P_2 P_3^* Fig. 6(c)), further confirming the climbing behavior of the upper part of the plume.

5. Mixed queue

5.1. Experiments

We consider a particular case of a mixed queue with $P : T = 2 : 1$. Assuming that the queue forms a regular sequence $\cdots PPTPPTPPT \cdots$, we examine the exhaust-gas dispersion from the component vehicles: P behind T, P behind P, and T. Three vehicles (two P's and one T) are placed in front of the gas-emitting vehicle. Although we did not confirm for each case, we suppose that the three preceding vehicles are sufficient to

produce wake turbulence equivalent to that of an infinite queue. Since the truck T generates longer wake (~1.5 car length, defined by the region of significant mean-flow deformation) than P does (~1 car length) but the spacing behind T is twice as large as that behind P, further addition of T in the preceding queue would make little difference in the wake turbulence. As in Section 3, two vehicles are set behind the gas-emitter. Therefore, the tested queues are: (i) $P_1P_2T_3P_4^*P_5T_6$, (ii) $P_1T_2P_3P_4^*T_5P_6$, (iii) $T_1P_2P_3T_4^*P_5P_6$.

Fig. 7 shows the concentration contours in the yz plane for the three cases. The dotted curves indicate the optimal fit to the Gaussian distribution:

$$\frac{Q}{2\pi U\sigma_y\sigma_z}\exp\left\{-\frac{(y-y_0)^2}{2\sigma_y^2}\right\}\left[\exp\left\{-\frac{(z-z_0)^2}{2\sigma_z^2}\right\}+\exp\left\{-\frac{(z+z_0)^2}{2\sigma_z^2}\right\}\right], \tag{1}$$

where the fitting parameters Q, σ_y, σ_z, y_0 and z_0 are determined by the Nelder–Mead simplex method ([4]). As shown in Section 4, a following P (e.g. P_5 in the queue (i)) raises the plume around the center $y=0$ and creates a bulge in the contours (e.g. Fig. 7(i-b)). Similar effect is produced by T in larger magnitude (Fig. 7(i-a), (ii-b)). This concentration increase around $y=0$, however, is not caused by the plume climbing over T; the concentration above T ($z=170$ mm) is found much lower than that of the outermost contours in Fig. 7. Instead, the bulge around $y=0$ is created by the roll-up wake flow behind T (cf. Fig. 5 of K1). Its effect is most clearly observed in Fig. 7(iii-c), where the plume is vertically elongated by the roll-up wake of the gas-emitting T_4^*. We note that the contours at low z behind T_4^* in the queue (iii) is approximately symmetric about $y=0$ in contrast to the significant shift toward the negative y (exhaust pipe position) for the case with an isolated T (cf. Fig. 8 of K1). This is the same effect as observed with P in Section 3.

Fig. 8 shows σ_y, σ_z and z_0 against x. The behavior of σ_y and σ_z can be sorted into two groups: relatively large σ_y and small σ_z when P emits the exhaust gas (solid and dashed lines), and relatively small σ_y and large σ_z when T emits the exhaust gas (dotted lines). When P emits the gas, the plume shape depends on the type of the following vehicle (see Fig. 7(i-a), (i-b), (ii-a), (ii-b)), but once fitted to the Gaussian formula, the gross plume size is almost independent of the type of the following vehicles. We remark that this is a mere coincidence, and different results would be obtained if we employed differently shaped vehicles. When T emits the gas, the plume is expanded in the vertical by the roll-up wake, resulting in large σ_z. The suppressed growth of σ_y in this case is probably due to the vertically biased turbulent fluctuations in the wake of T. Similar effect is observed in Fig. 8(a) where the early growth rate of σ_y is larger for $P_1T_2P_3P_4^*T_5P_6$ (dashed line) than for $P_1P_2T_3P_4^*P_5T_6$ (solid line), the former-case P^* being behind a P whereas the latter-case P^* being behind a T.

The plume height z_0 is zero except for Fig. 7(iii-b) where the plume lifting effect of T_4 and P_5 overcomes the vertical mixing that tends to lower the plume axis.

5.2. Combined effect

The experiments revealed the concentration field when one of the vehicles emit the exhaust gas. Now, we estimate the concentration field when all the vehicles emit the gas at the same time.

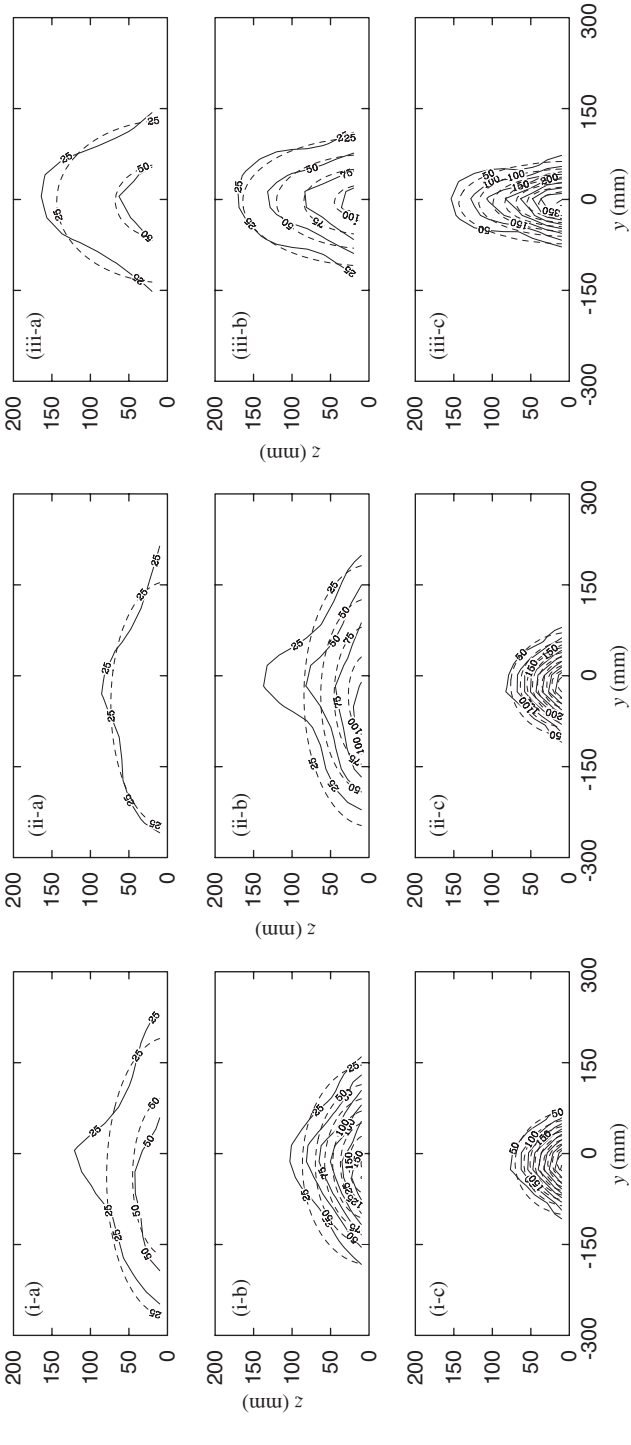

Fig. 7. Concentration contours in the yz plane for the mixed queues: (i) $P_1P_2T_3P_4^*P_5T_6$, (ii) $P_1T_2P_3P_4^*T_5P_6$, (iii) $T_1P_2P_3T_4^*P_5P_6$. The solid lines are the measured data and the dashed lines are the optimal fit to the Gaussian formula (1). The x (mm) coordinates are (i-a) −1954 (behind T_6), (i-b) −1050 (behind P_5), (i-c) −525 (behind P_4^*), (ii-a) −2354 (behind P_6), (ii-b) −1229 (behind T_5), (ii-c) −525 (behind P_4^*), (iii-a) −1829 (behind P_5), (iii-b) −1124 (behind T_4^*), (iii-c) −604 (behind T_4^*).

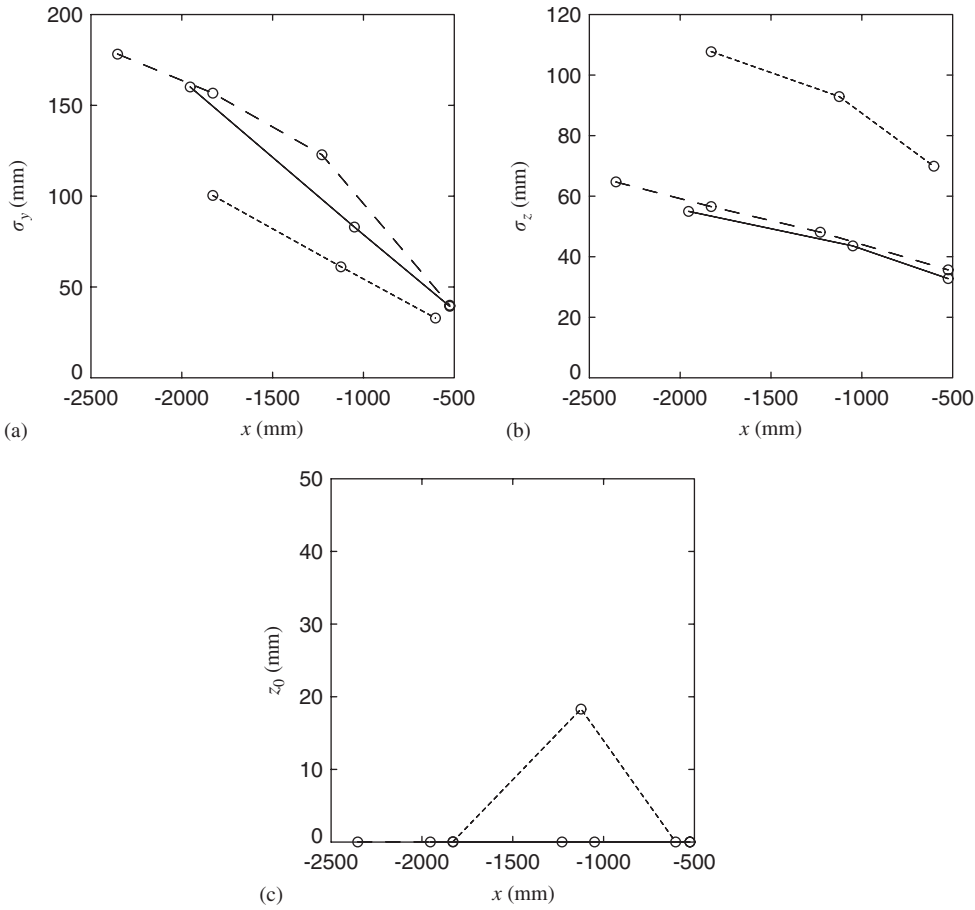

Fig. 8. The Gaussian fitting parameters σ_y, σ_z and z_0 in Eq. (1) for the mixed queue experiments. Solid line: $P_1P_2T_3P_4^*P_5T_6$, dashed line: $P_1T_2P_3P_4^*T_5P_6$, dotted line: $T_1P_2P_3T_4^*P_5P_6$.

First, we approximate the contribution from one vehicle by a single Gaussian formula. In the previous section, we fitted the Gaussian formula (1) to the concentration field individually at a few x points. As shown in Fig. 8(a), (b), the plume widths σ_y and σ_z grow approximately in proportion to x. If we extrapolate the trends in Fig. 8(a), (b) toward larger x (to the right), we find that the intercepts with the x-axis are ahead of the tailpipe exit ($x = -217.5$ mm for P and $x = -283$ mm for T). This is due to the rapid dispersion of the exhaust gas in the wake of the vehicles. Accounting for this effect, we write the widths of the plume from a vehicle with the front bumper at $x = x_0$ as

$$\sigma_y = \alpha(x_0 + x_\alpha - x), \quad \sigma_z = \beta(x_0 + x_\beta - x), \tag{2}$$

where x_α and x_β are the intercept coordinates with the x-axis in Fig. 8(a) and (b), respectively. The values of α, β, x_α and x_β are obtained by the least-squares fit to the data in Fig. 8(a), (b). The results are listed in Table 1.

Table 1
Plume parameters for the relevant cases

Configuration	α	x_α (mm)	β	x_β (mm)
(i) $P_1P_2T_3P_4^*P_5T_6$	0.085	−64	0.015	1699
(ii) $P_1T_2P_3P_4^*T_5P_6$	0.075	177	0.016	1774
(iii) $T_1P_2P_3T_4^*P_5P_6$	0.055	−10	0.030	1785
$P_1P_2P_3^*P_4P_5$	0.087	−39	0.004	7825
Bare-pipe P	0.019	287	0.007	930
Bare-pipe T	0.015	59	0.012	111

In the configuration column, the Roman numbers correspond to those in Fig. 7.

For simplicity, $y_0 = z_0 = 0$ is assumed in the Gaussian formula (1). Then, the concentration field $C(x, y, z)$ by a vehicle is written as

$$C(x,y,z) = \frac{Q}{\pi\sigma_y\sigma_z U}\exp\left(-\frac{y^2}{2\sigma_y^2}-\frac{z^2}{2\sigma_z^2}\right). \tag{3}$$

Now, we consider an infinite sequence of vehicles at an interval l (head-to-head). Then, at x ($<l$), the total contribution from the preceding vehicles at $x_0 = il$ ($i = 1, 2, \ldots$) becomes

$$C(x,\,y,\,z) = \frac{Q}{\pi\alpha\beta U}\sum_{i=1}^{\infty}\frac{1}{(il+x_\alpha-x)(il+x_\beta-x)}\exp\left(-\frac{y^2}{2\sigma_y^2}-\frac{z^2}{2\sigma_z^2}\right). \tag{4}$$

Here, we assumed that α and β are constant. This assumption is not correct since the growth rate of the plume width should decrease as the plume propagates downstream. Hence, α and β are overestimated and thus the concentration is underestimated. Nonetheless, the error by this assumption is small because the concentration decays rapidly as the inverse square of x as evinced by the fact that the concentration behind the second following vehicle is only about 10% of the near-source value (see Fig. 7).

The coordinate $x_0 = l$ of the vehicle immediately in front of the measurement point x belongs to the head of the vehicle, not to the tailpipe exit. Hence, the region where the plume from the immediately preceding vehicle affects but the plume of the immediately following vehicle does not is $-d < x < l - d$. Taking the average of (4) from $x = -d$ to $l - d$, we obtain the x-independent line-source concentration field $\overline{C}(y, z)$ as

$$\begin{aligned}\overline{C}(y,\,z) &= \frac{Q}{\pi\alpha\beta U}\sum_{i=1}^{\infty}\frac{1}{l}\int_{-d}^{l-d}\frac{1}{(il+x_\alpha-x)(il+x_\beta-x)}\exp\left(-\frac{y^2}{2\sigma_y^2}-\frac{z^2}{2\sigma_z^2}\right)\mathrm{d}x\\ &= \frac{q}{\pi\alpha\beta U}\int_{d}^{\infty}\frac{1}{(x+x_\alpha)(x+x_\beta)}\exp\left\{-\frac{y^2}{2\alpha^2(x+x_\alpha)^2}-\frac{z^2}{2\beta^2(x+x_\beta)^2}\right\}\mathrm{d}x,\end{aligned} \tag{5}$$

where we defined the line-source strength $q = Q/l$.

The integration of (5) must be done numerically except when $x_\alpha = x_\beta = d = 0$, in which case we obtain

$$\overline{C}(y,\,z) = \frac{q}{\pi\alpha\beta U}\frac{\sqrt{\pi}}{2}\frac{1}{\sqrt{B}}, \tag{6}$$

where

$$B = \frac{y^2}{2\alpha^2} + \frac{z^2}{2\beta^2}.$$

As shown in Fig. 9, the mixed queue consists of three types of vehicles P_a, P_b and T. The distance between the vehicles of the same type is l for all the types. For the source strength q, of which only the relative magnitude are necessary, we adopt the typical NO_X emission factor in Japan ([5]):

$$q_p = 0.22\,\mathrm{g/km}, \quad q_t = 0.76\,\mathrm{g/km}, \tag{7}$$

where the subscripts p and t denote the passenger car P and the truck T, respectively. Since the contribution from each of the types is expressed as a line source (5), the total contribution $\overline{C}_m$ from the three types can be calculated as a simple sum of the three line sources:

$$\overline{C}_m = \overline{C}_{P_a} + \overline{C}_{P_b} + \overline{C}_T. \tag{8}$$

Further, we approximate $\overline{C}_m$ by a Gaussian line source:

$$\overline{C}_m \sim \frac{q_m}{\pi\alpha_m\beta_m U}\frac{\sqrt{\pi}}{2}\frac{1}{\sqrt{B_m}}, \tag{9}$$

where $q_m = 2q_p + q_t$ and the subscript m stands for 'mixed queue'. The optimal values of α_m and β_m are obtained by minimizing the rms of the difference between the two sides in Eq. (9) at grid points in $10 \leqslant y, z\,(\mathrm{mm}) < 200$. The result is

$$\alpha_m = 0.049, \quad \beta_m = 0.038. \tag{10}$$

Similar procedure is applied to a queue composed only of passenger cars. The optimal values α_p and β_p for this case become

$$\alpha_p = 0.057, \quad \beta_p = 0.015. \tag{11}$$

The mixed queue has relatively small α and large β because of the large emission factor of T whose exhaust plume has relatively small σ_y and large σ_z (see Fig. 7(iii)).

The above values of α and β are a little overestimate because the experiments were conducted in the presence of the boundary layer on the table top, which does not exist on the real road when there is no ambient wind. The boundary layer tends to spread the plume

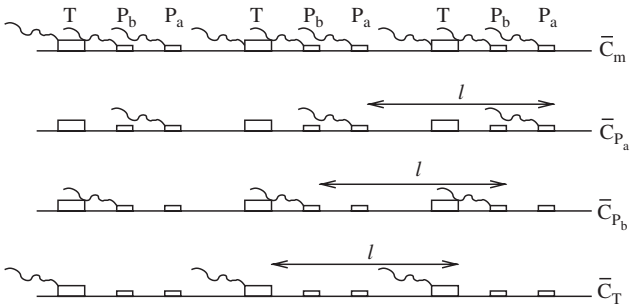

Fig. 9. Conceptual sketch of the mixed queue. Emission from P_a, P_b and T correspond to the configurations $P_1P_2T_3P_4^*P_5T_6$, $P_1T_2P_3P_4^*T_5P_6$ and $T_1P_2P_3T_4^*P_5P_6$, respectively.

especially in the spanwise (y) direction (cf. Fig. 9 of K1). The effect can also be observed in Figs. 4 and 7 as slight expansion of the contours near $z = 0$.

One method of canceling the effect of the boundary layer is to evaluate the increase of the growth rates α, β from the bare-pipe case. If we assume that the effect of the boundary layer is equivalent for both the vehicle-queue and the bare-pipe experiments, the difference in the growth rates are attributable solely to the mixing by the vehicle queue. This assumption is not strictly correct since the vehicle wake interact non-linearly with the floor boundary layer. However, at the leading order, the assumption should provide a reasonable approximation.

We choose as reference the combined buoyant plume from the bare pipes when the vehicle bodies are removed from the vehicle queue. The effective growth rates α^{pipe} and β^{pipe} are obtained by the same procedure as for the vehicle queue. The relevant parameters of the single bare-pipe plumes are shown in Table 1. In the calculation for the mixed queue of $P : T = 2 : 1$, the height z_0 of the component plumes is set as the tailpipe height (9 and 25 mm for the P- and T-type plumes, respectively), and that of the combined plume is set as the emission-weighted height $(9 \times 2q_{\text{p}} + 25 \times q_{\text{t}})/(2q_{\text{p}} + q_{\text{t}}) = 19$ mm. The result is

$$\alpha_{\text{m}}^{\text{pipe}} = 0.016, \quad \beta_{\text{m}}^{\text{pipe}} = 0.010, \tag{12}$$

$$\alpha_{\text{p}}^{\text{pipe}} = 0.018, \quad \beta_{\text{p}}^{\text{pipe}} = 0.0075. \tag{13}$$

Now, we relate the growth rates α and β to the eddy diffusivity. Using the eddy diffusivity (K_x, K_y, K_z), the Robert solution ([6]) for the concentration field becomes

$$C = \frac{Q}{4\pi(K_y K_z)^{1/2} R} \exp\left\{-\frac{U}{2K_x}(R - x)\right\}, \tag{14}$$

where $R^2 = x^2 + (K_x/K_y)y^2 + (K_x/K_z)z^2$. By comparing (14) with the Gaussian formula (1), we find $K_y \sim \frac{1}{2}\alpha^2 U|x|$, $K_z \sim \frac{1}{2}\beta^2 U|x|$ in the core region of the plume. Hence, we obtain

$$\frac{K_{y,\text{m}}}{K_{y,\text{m}}^{\text{pipe}}} \sim 9, \quad \frac{K_{z,\text{m}}}{K_{z,\text{m}}^{\text{pipe}}} \sim 10, \tag{15}$$

$$\frac{K_{y,\text{p}}}{K_{y,\text{p}}^{\text{pipe}}} \sim 10, \quad \frac{K_{z,\text{p}}}{K_{z,\text{p}}^{\text{pipe}}} \sim 4. \tag{16}$$

The exact values depend on the employed assumptions and approximations, but we may conclude that the wake of the mixed vehicle queue increases the eddy diffusivity by a factor of about 10 and that the absence of trucks reduces vertical dispersion considerably.

6. Summary and discussion

In a reduced-scale wind-tunnel experiment, we studied the dispersion behavior of automobile exhaust gas in various configurations of vehicle queues. For the chosen vehicle types and intervals, we found the following.

(1) For a queue consisting only of passenger cars (P), two preceding P's are sufficient to generate wake turbulence equivalent to that by infinite number of preceding P's. The wake turbulence of the preceding vehicles makes the concentration field at low z nearly symmetric for both P and T despite the laterally offset tailpipe position.

(2) A following P expands the exhaust plume mostly in the horizontal, but also scoops up the oncoming plume around the centerline ($y = 0$) of the vehicle body.
(3) A following truck (T) spread the plume vertically by the roll-up wake behind the body in addition to horizontal expansion by blocking the path of the oncoming plume.
(4) In a mixed queue of $P : T = 2 : 1$, the expansion behavior of the exhaust plume depends primarily on the type of the gas-emitting vehicle: $\sigma_y > \sigma_z$ when P emits the gas, and $\sigma_y \sim \sigma_z$ when T emits the gas.
(5) The concentration in the mixed queue when all the component vehicles emit the exhaust gas can be estimated by approximating the contributions from different types of gas emitters by uniform line sources, and then superposing them. From the resulting growth rate of the plume width, we estimate that the vehicle queue increases the eddy diffusivity by a factor of about 10.

Our ultimate goal is to incorporate the effect of traffic-produced turbulence into air pollution models. In this respect, our current results are not satisfactory since they are valid only in a special condition of quiescent ambient. However, since high pollutant concentration occurs in calm-wind conditions, our results can be used to estimate the maximum possible concentration. In order to obtain the dispersion parameters for general conditions, further experiments need to be conducted, preferably on a moving belt to eliminate the floor boundary layer.

A caveat is that, in our experiments, the turbulent boundary layer on the table top enhances dispersion particularly in the lateral direction. Hence, the values of σ_y and σ_z obtained in our experiments should not be simply scaled up to the real situation. For this reason, our discussion has been mostly confined to qualitative features, and the quantitative analysis of Section 5.2 emphasizes possible errors due to unverified assumptions.

Our experiments are unique in that the bulk parameters such as the multiplication factor for the eddy diffusivity are obtained from the detailed study of exhaust dispersion by individual vehicles. In contrast, most air pollution models (e.g. [7–9]) postulate some formulae that represent the effect of the moving traffic, and find the relevant parameters by optimal fit to field observations. Since such an empirical approach cannot separate the effects of co-existing factors such as ambient turbulence and thermal stratification, the obtained parameter values are somewhat uncertain. However, because such parameters are where ours and the empirical approaches meet, the results of our experiments could be used as a validation of the previously applied model parameters. Unfortunately, since existing models neglect diffusion of the exhaust gas from bare pipes in a quiescent ambient and hence the multiplication factor for the eddy diffusivity is infinity, direct comparison with our results is difficult at present.

Acknowledgments

This research was conducted as a project of Petroleum Energy Center with a financial support by Japanese Ministry of Economy, Trade and Industry. We appreciate the technical assistance of Mr. T. Kawata at Forum Engineering Inc.

References

[1] P.E. Benson, A review of the development and application of the CALINE3 and 4 models, Atmos. Environ. 26B (1992) 379–390.

[2] R. Berkowicz, OSPM—a parameterised street pollution model, Environ. Monit. Assessment 65 (2000) 323–331.
[3] G.T. Csanady, Turbulent Diffusion in the Environment, D. Reidel Publishing Co., Dordrecht, 1973.
[4] R.E. Eskridge, J.C.R. Hunt, Highway modeling. Part I: prediction of velocity and turbulence fields in the wake of vehicles, J. Appl. Meteorol. 18 (1979) 387–400.
[5] M. Galassi, J. Davies, J. Theiler, B. Gough, G. Jungman, M. Booth, F. Rossi, GNU Scientific Library: Reference Manual, second ed, Network Theory Ltd, 2003.
[6] Japan Environment Agency, A survey on emission factors and the gross amount of automobile exhaust gas. Technical Report (1998).
[7] I. Kanda, K. Uehara, Y. Yamao, Y. Yoshikawa, T.A. Morikawa, wind-tunnel study on exhaust-gas dispersion from road vehicles—Part I: velocity and concentration fields behind single vehicles, J. Wind Eng. Ind. Aerodyn., in press, doi:10.1016/j.jweia.2005.12.003.
[8] A.G. Venetsanos, J.G. Bartzis, S. Andronopoulos, D. Vlachogiannis, Vehicle effects on street canyon air pollution pattern, in: Ninth International Conference on Modeling, Monitoring and Management of Air Pollution, WIT Press, Southampton, 2001, pp. 193–202.
[9] R.J. Yamartino, G. Wiegand, Development and evaluation of simple models for the flow, turbulence and pollutant concentration fields within an urban street canyon, Atmos. Environ. 20 (1986) 2137–2156.